Rare Met. (2019) 38(11):1078–1085
https://doi.org/10.1007/s12598-018-1152-5

RARE METALS
www.editorialmanager.com/rmet

Tribological behavior of a Ni-WS_2 composite coating across wide temperature ranges

Shuai Cui, Wen-Sheng Li*, Ling He, Li Feng, Guo-Sheng An, Wei Hu, Chun-Xia Hu

Received: 8 March 2017 / Revised: 11 April 2017 / Accepted: 27 August 2018 / Published online: 20 November 2018
© The Nonferrous Metals Society of China and Springer-Verlag GmbH Germany, part of Springer Nature 2018

Abstract In order to reduce the friction coefficient of a pure nickel coating and extend the lifetime of metal parts under extreme friction conditions, a series of Ni-based WS_2-composite solid lubrication coating containing different WS_2 concentrations were prepared on a 45# mild carbon steel substrate by electroplating. The cyclic voltammetry method was used to investigate the electroplating regulation of the Ni-WS_2 composite coatings. X-ray diffraction (XRD) and scanning electron microscopy (SEM) were used to analyze the microstructures and wear surfaces of the composite coatings, the tribological properties and wear mechanisms of the composite coatings with different WS_2 concentrations. The results show that the addition of WS_2 can promote the cathode polarization of the electroplating process, and the polarization degree goes up with the increase in WS_2 concentrations. The friction coefficient of Ni-composite coatings significantly decreases by the addition of WS_2 particles. The lowest friction coefficient at room temperature is obtained at a value around 0.01–0.03 from the coating deposited in the electrolyte solution with a 30 $g \cdot L^{-1}$ WS_2 concentration. The friction coefficient of the Ni-WS_2 composite coating remains in 0.01–0.03 with the increase in temperature from room temperature to 300 °C. When the temperature goes up to 500 °C, the friction coefficient manifests a continuous increase to 0.12, because WS_2 is gradually oxidized into WO_3 and therefore loses its lubrication ability.

Keywords WS_2; Self-lubricating composites coating; Frictional wear; Temperature

1 Introduction

Surface coatings play an important role in prolonging the lifetime of components by enhancing the surface mechanical performance. Owing to varying environments, it is unavoidable that areas with intermittent contact are worn faster than areas with less contact, which may result in pre-failure, catastrophic damage or loss [1]. Thus, it is important to find solid lubricant materials that exhibit and maintain a reduced friction coefficient under harsh conditions including vacuums, high speeds and even high temperatures. Examples of applications requiring such materials in extreme environments include bearings and bushings for space satellites and vehicles [2–4]. A solid lubricant can solve these problems for sliding parts with low friction under dry conditions mostly in the aerospace industry through incorporating coatings with some transition metal disulfides with a low friction such as MoS_2 [5–7], WS_2 [8–10], graphite and boron nitride [11–13]. To overcome deficiencies such as low hardness of single solid lubricant coating, a strategy of combining the functions of pure nickel has been proposed. Electroless pure nickel coatings have been widely used in the chemical, mechanical and electronic industries because of their high hardness and abrasion resistance [14]. These composite coatings include both soft and hard particles simultaneously to achieve the wear resistance and lubrication characteristics of a single layer.

S. Cui, W. Hu, C.-X. Hu
School of Materials Science and Engineering, Lanzhou University of Technology, Lanzhou 730050, China

W.-S. Li*, L. He, L. Feng, G.-S. An
State Key Laboratory of Advanced Processing and Recycling of Nonferrous Metals, Lanzhou University of Technology, Lanzhou 730050, China
e-mail: wensheng-li@sohu.com

Tungsten disulfide (WS_2) possesses a layered structure with good lubrication property, and it provides strong adhesion to the substrate. The present research focused on using sputtering method to develop a Ni coating embedded with WS_2 to be used to reduce the wear condition of coatings. Sun et al. [15] used sputtering method to prepare MoS_2/WS_2 multilayer thin films and found that the film exhibited a much lower friction coefficient and longer lifetime compared to a single film. WS_2/MoS_2/C composite films were prepared in an Ar/C_2H_2 atmosphere by magnetron reaction sputtering by Zhou et al. [16], which expanded the application of WS_2/MoS_2 films under humid conditions. Sputtering method is restricted by the target material and unsuited for large area deposition. Electroplating is one of the effective ways to improve the performance of lubrication, coating wear resistance and corrosion resistance, while electroplating has the advantages of high density, low porosity and flexible methodologies. This work aimed at electroplating a wide-temperature, self-lubricating Ni-WS_2 composite coating that will possess high hardness combined with good lubrication properties.

2 Experimental

All chemicals were analytical grade to minimize the effect of impurities. The electrolyte solution for nickel plating contained $NiSO_4 \cdot 6H_2O$ (250 $g \cdot L^{-3}$), $NiCl_2 \cdot 4H_2O$ (45 $g \cdot L^{-3}$) and H_3BO_3 (40 $g \cdot L^{-3}$) in distilled water. The pH for the plating bath was adjusted by H_2SO_4 or NaOH to 4.0 ± 0.5, because this value can induce the lowest internal stress during Ni electroplating [17, 18]. The electrolyte solution was stirred in a multi-position magnetic stirrer. The solid WS_2 lubricant particles were 3–5 μm in diameter. Cetyl trimethyl ammonium bromide (CTAB) was added to the electrolyte solution with 0, 10, 20, 30 and 40 $g \cdot L^{-1}$ WS_2 particles, and the corresponding mass ratio of CTAB/WS_2 is 0.02.

45# mild carbon steel plate was chosen for the electroplating substrate. Prior to deposition, the substrate was sand-blasted followed by alkaline solution flushing using 6 g NaOH, 2 g Na_2CO_3, 3 g Na_3PO_4 and 1 g Na_2SiO_3. The substrate was immersed into 50% HCl solution for 30 s and then rinsed with distilled water. A pure nickel plate was used as the anode. The electroplating was performed with a DF-101S magnetic stirrer at 50 °C and a current density of 4 $A \cdot L^{-2}$ for 90 min to produce Ni-WS_2 composite coating.

Cyclic voltammetry (CV) method was used in a CS electrochemical workstation to determine a suitable potential range for the reduction reaction. The working electrode was an Φ3-mm glassy carbon electrode. The counter electrode was a platinum electrode. A saturated calomel electrode (SCE) was used for the reference electrode. The morphology of the composite coatings was observed using a Quanta 450 FEG scanning electron microscope (SEM). The phase compositions of the wear debris were detected by a Renishaw's inVia micro-Raman spectrometer with a laser wavelength of 514 nm. The three-dimensional contours of the composite coating were characterized by laser scanning confocal microscopy (LSCM, C2 Plus, Nikon, Japan). The macro-hardness of the composite coating was measured using HRS-150 hardness tester with a load of 0.98 N and a dwell time of 10 s. The microstructures of the coatings were characterized by X-ray diffractometer (XRD, Bruker D8). The reported macro-hardness values were the average of at least five measurements on different locations around the center section of each composite coating.

A reciprocating HT-1000 high-temperature wear tester (Fig. 1) was used to evaluate the friction behaviors at 25, 100, 200, 300, 400 and 500 °C, and 6-mm-diameter GCr 15 steel balls with hardness of HRC (62-66) were used as the counter body. A constant load of 20 N was applied in all tests, and the running time was 10 min for the Ni-WS_2 composite coating. The sliding frequency was 5 Hz, and the sliding stroke was 5 mm. The wear volume was calculated using the integral method.

3 Results and discussion

3.1 Deposition rate curve for composite coating

Figure 2 shows WS_2 and Ni concentrations in the composite coatings as a function of WS_2 bath concentration. The increase of WS_2 concentrations with the increase in WS_2 bath concentrations indicates an increasing co-deposition of WS_2 into the coating. The co-deposition of WS_2 particles depends on the number of collisions between the particles and cathode. Then, the inert WS_2 particle is attracted to the cathode due to the applied voltage in the electroplating process. In the high WS_2 bath concentration region, the increments of WS_2 bath concentration alleviate the collision effect between the particles and the cathode. Thus, WS_2 content of the composite coating increases slightly [19]. Figure 2 also shows that with the increase in WS_2 bath concentration, Ni concentration decreases. The deposition rate curve further explains that with the increase in WS_2 bath concentration, an increasing number of WS_2 particles preferentially occupy the position of Ni crystal to inhibit the crystallization of nickel in the process of electrochemical deposition.

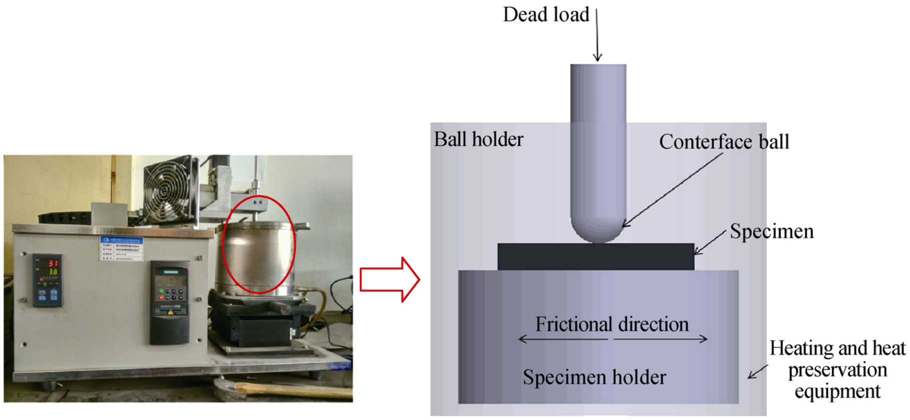

Fig. 1 A schematic representation of reciprocating wear tester apparatus

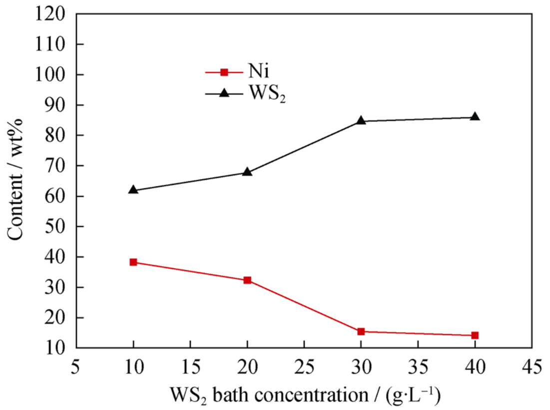

Fig. 2 WS_2 and Ni concentrations of coatings versus WS_2 bath concentration

3.2 Morphology and phase of composite coating

3.2.1 *Morphology of composite coating*

Figure 3 shows SEM images of surfaces and cross section, and LSCM images of surface profile of the composite coatings with different WS_2 concentrations. It can be seen that after deposition, many WS_2 particles are incorporated into the deposition matrix with Ni. When CTAB keeps within 20 $mg \cdot g^{-1}$ WS_2 specified proportion, with the increase in WS_2 concentration, the coating surface becomes smooth. The porosity and particle reunion phenomenon are reduced. However, when WS_2 concentration is 30 $g \cdot L^{-1}$, the coating surface is the best (Fig. 3d). Because WS_2 particles have a negative surface charge, cationic surfactants like CTAB will be easily adsorbed on the suspended particle [20]. Therefore, a net positive charge is formed through the adsorption of cationic surfactants that inhibit the formation of particle clusters and lead to more stable particle suspension in the bath [21]. With the addition of more surfactant, the electric double layer formatting on the particle is compressed and the dispersion stability is poor [22]. As shown in Fig. 3e, when WS_2 concentration is 40 $g \cdot L^{-1}$, the smoothness of Ni-WS_2 composite coating surface gradually becomes worse.

3.2.2 *Phase of composite coating*

XRD patterns of Ni and Ni-WS_2 composite coating are shown in Fig. 4. It can be seen that pure Ni coating is a crystalline structure and does not contain another phase. The main crystal planes of the pure Ni coating are (111), (200) and (220). With the addition of WS_2 particles to the coating, XRD pattern appears WS_2 diffraction peaks, such as (002), (004), (103) and (006). With the increase in WS_2 concentration, (002) diffraction peak intensity gradually increases and demonstrates the changing trend in WS_2 content in the coating. However, (111) diffraction peak intensity gradually weakens because WS_2 particles have a pinning effect on the nickel crystal boundary and can inhibit the crystallization of nickel.

3.3 CV curves of composite coating

CV curves for Ni-WS_2 composite in electrodeposition baths are plotted and are shown in Fig. 5, in which the electrochemical performance of the electrodes in the plating baths was characterized. It is evident that there is a reduction peak as the potential becomes more negative, and this peak means that Ni^{2+} is reduced to Ni^{+} or Ni [23]. The reduction potential of nickel is about − 1.6 V through the experiments. With the addition of WS_2, the reduction potential becomes increasingly negative, because the adsorption of WS_2 particles is in competition with Ni crystal growth. An increasing number of WS_2 particles adsorbing CTAB preferentially occupy the position of Ni crystal with the increase in WS_2 concentration, which increases the real area of the electrode surface, and the local current density of the electrode surface decreases, and

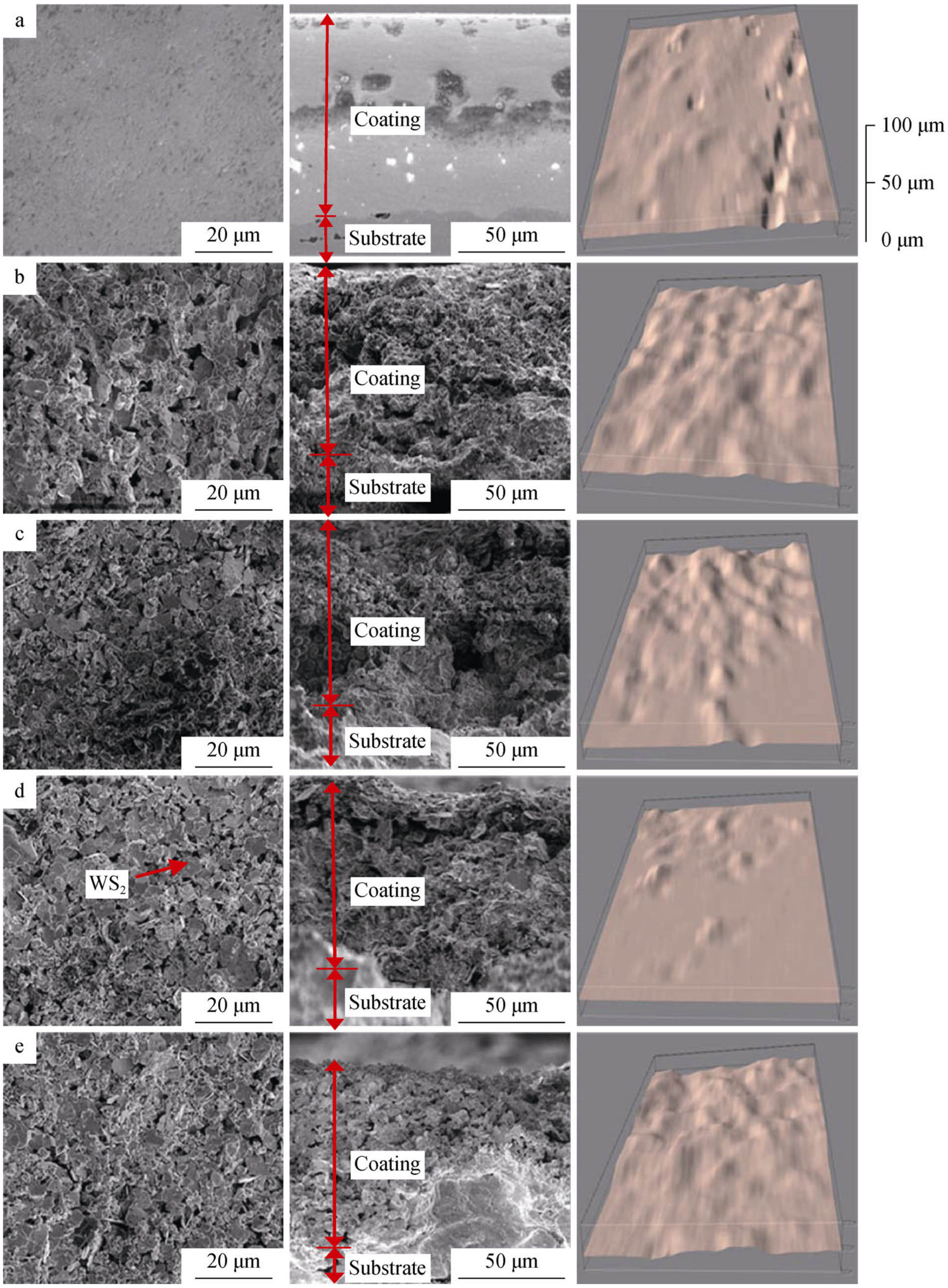

Fig. 3 SEM images of surface, cross section and LSCM images of surface profile of Ni electrodeposition at different WS_2 concentrations: **a** 0 g·L^{-1}, **b** 10 g·L^{-1}, **c** 20 g·L^{-1}, **d** 30 g·L^{-1} and **e** 40 g·L^{-1}

the cathode diffusion length increases [23]. Thus, the deposition of nickel ions in the cathode surface requires more polarization, as the cathode electrode potential becomes increasingly negative.

3.4 Mechanical and tribological properties of composite coating

Figure 6 illustrates the friction coefficient of Ni and Ni-WS_2 composite coatings at different WS_2 bath concentrations at 25 °C. It is observed that the friction coefficient of the pure Ni coating is nearly 12 times that of Ni-WS_2 composite coating, and with the increase in WS_2 concentration, the friction coefficient gradually decreases. The lowest friction coefficient at room temperature is obtained from the coating deposited in the electrolyte solution with a WS_2 concentration of 30 g·L^{-1}, because WS_2 concentrations in the composite coating rise with increase in particle concentrations in the bath. The lamellar structure existing in the WS_2 particles crystallites is helpful

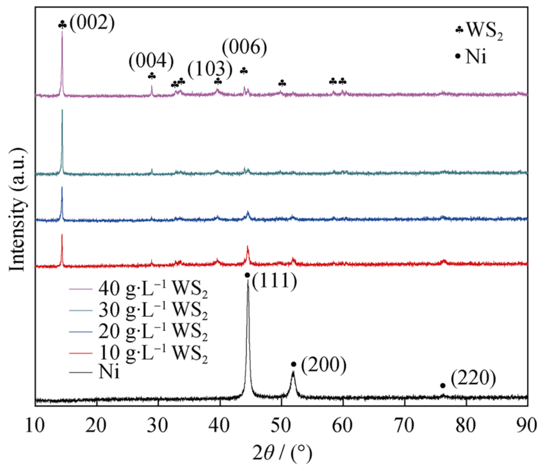

Fig. 4 XRD patterns of Ni and Ni-WS$_2$ composite coatings at different WS$_2$ bath concentrations

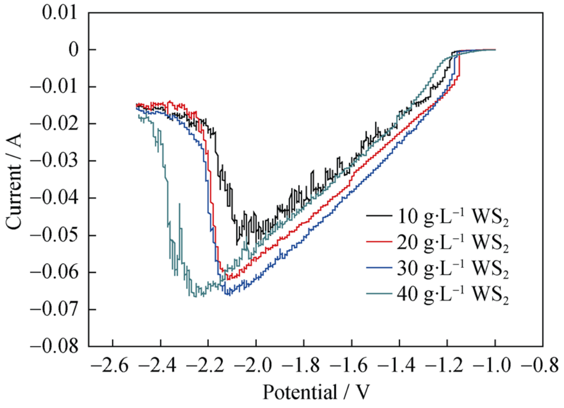

Fig. 5 CV curves of Ni-WS$_2$ coating

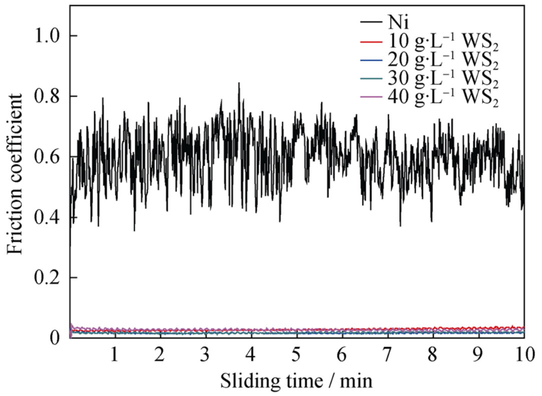

Fig. 6 Friction coefficient of Ni and Ni-WS$_2$ composite coatings at different WS$_2$ bath concentrations at 25 °C

for sliding. Thus, WS$_2$ grinding produced by wear can easily form transfer film during the process of friction to avoid direct contact between the metals, thereby reducing the friction coefficient [24–27]. However, if WS$_2$ concentrations are excessive, the thickness of the transfer film will increase and lead to molecular accumulation of the lubricating agent to produce viscoelastic resistance, and thus, the friction coefficient increases [28].

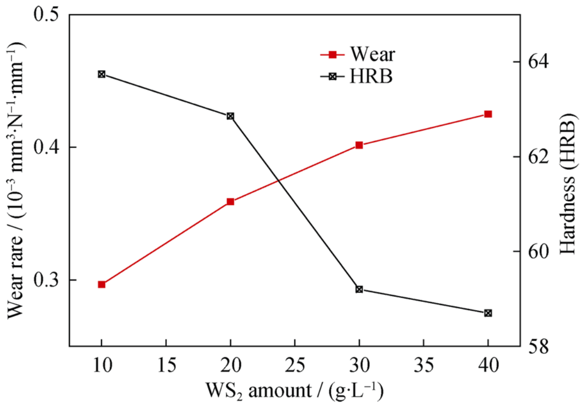

Fig. 7 Wear rates and macro-hardness for Ni-WS$_2$ composite coatings as a function of WS$_2$ bath concentration

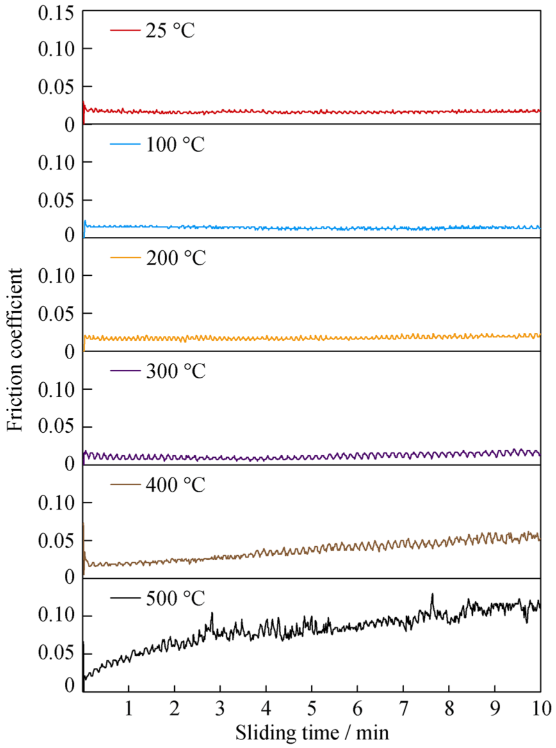

Fig. 8 Friction curves for Ni-30 g·L^{-1} WS$_2$ composite coatings at different temperatures

Wear rates and the macro-hardness of Ni-WS$_2$ composite coatings at different WS$_2$ bath concentrations are shown in Fig. 7. The results show that the wear rate of the composite coating is the inverse of the macro-hardness. It is clear that WS$_2$-co-deposited particles reduce the wear resistance. As the amount of WS$_2$ in the coating increases, the coating wears out more easily because of the soft nature of WS$_2$, resulting in a low macro-hardness.

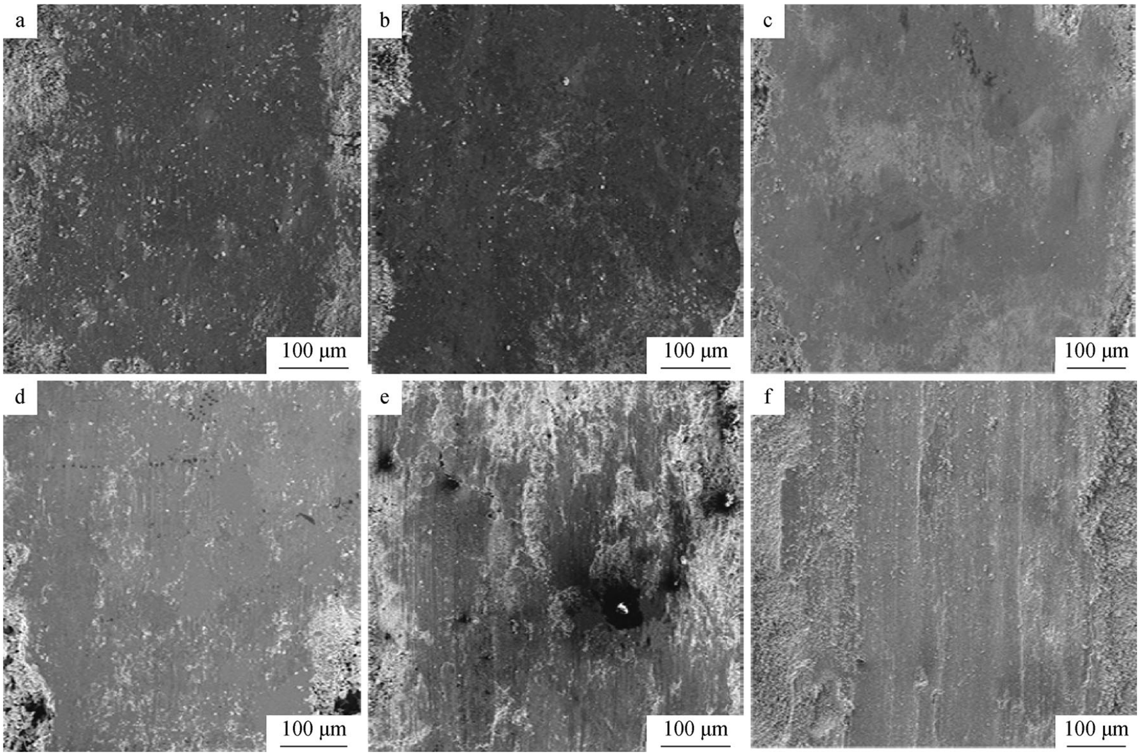

Fig. 9 SEM images of worn surface of Ni-30 g·L^{-1} WS_2 composite coatings at different temperatures: **a** 25 °C, **b** 100 °C, **c** 200 °C, **d** 300 °C, **e** 400 °C and **f** 500 °C

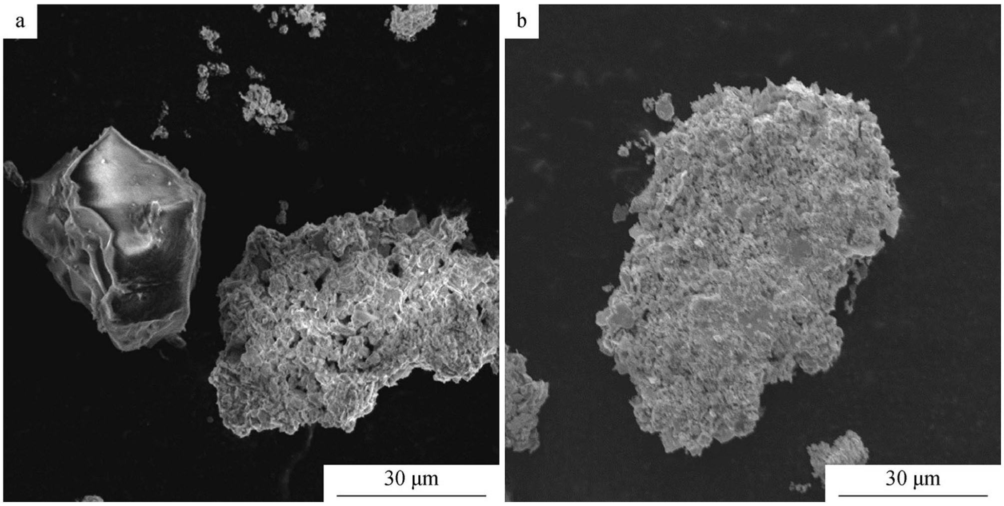

Fig. 10 SEM images of different wear debris at 500 °C

The typical friction curves for Ni-30 g·L^{-1} WS_2 composite coatings at different temperatures are shown in Fig. 8. Within 25–300 °C, the friction coefficient value slightly decreases and then rises within 400–500 °C. Figure 9 shows SEM images from worn surfaces of Ni-30 g·L^{-1} WS_2 composite coating at different testing temperatures. Small grooves, small flaking pits and micro-cracks can be found on the worn surfaces of the composite coating, and the worn surfaces of the composite coating get smooth gradually with temperature changing from 25 to 300 °C; but for the big grooves, the flaking off is more severe at 400 and 500 °C, as shown in Fig. 9e, f. To understand the wear mechanism of Ni-WS_2 composite coating, a series of SEM observation are obtained. Figure 10a, b show SEM images of the wear debris at 500 °C. As can be seen, there are pieces of coating coming off, and

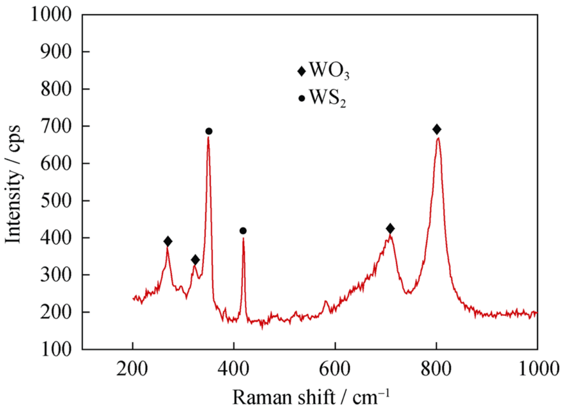

Fig. 11 Raman spectrum of worn Ni-WS$_2$ surfaces at 500 °C

the presence of large particles can be seen. Consequently, the main wear mechanism of the composite is fatigue delaminating.

The reason that the friction coefficient slightly drops within 25–300 °C is that with the increase in temperature, the molecules are encouraged to move; therefore, the transfer film is speeded up to form and prevent direct contact between the metal materials to reduce the friction coefficient [29]. In addition, WS$_2$ particle is very sensitive to the atmospheric environment, and the friction coefficient of WS$_2$ significantly increases in a damp environment [30]. Therefore, when there is an increase in temperature, the air humidity reduces, and then the friction coefficient drops significantly.

The friction coefficient goes up at 400–500 °C, because WS$_2$ will gradually be oxidized into WO$_3$ at 425 °C [31], and there is degradation in lubrication performance. To further demonstrate the presence of WO$_3$ at 500 °C, the phase constituents of wear debris were examined through Raman spectrum, as shown in Fig. 11. The main phase is WO$_3$, and it is documented that a composite coating with this phase is harmful to the lubrication performance [31]. Thus, the worn surfaces of the composite coating can be found in the grievous grooves, as shown in Fig. 9f.

4 Conclusion

In this study, electrochemical deposition of a Ni-WS$_2$ self-lubricating composite coating results in a remarkable self-lubricity and lower friction coefficient at a value around 0.01–0.03, compared with a pure Ni coating. With a 30 g·L^{-1} WS$_2$ concentration, the Ni-WS$_2$ composite coating has the lowest friction coefficient. The Ni-WS$_2$ composite coating presents remarkable self-lubricity over a wide temperature range from 25 to 300 °C. At over 400 °C, the WS$_2$ will gradually be oxidized into WO$_3$ and lose its lubricating ability. The reduction potential for Ni ions becomes increasingly negative with the increase in WS$_2$ concentration. This is explained by that WS$_2$ particles adsorb CTAB preferentially to occupy the position of the Ni crystal, promoting the cathode polarization.

Acknowledgements This study was financially supported by International Science and Technology Cooperation Program of China (No. 2015DFR51090) and the Supporting Program of Gansu Province (No. 1604WKCA008).

References

[1] He Y, Wang SC, Walsh FC, Li WS, He L, Reed PAS. The monitoring of coating health by in situ luminescent layers. RSC Adv. 2015;5(53):42965.

[2] Guo YX, Liu QB, Zhou F. Microstructure and wear resistance of high-melting-point AlCrFeMoNb$_x$TiW high-entropy alloy coating by laser cladding. Chin J Rare Met. 2017;41(12):1327.

[3] Aouadi SM, Singh DP, Stone DS, Polychronopoulou K, Nahif F, Rebholz C, Muratore C, Voevodin AA. Adaptive VN/Ag nanocomposite coatings with lubricious behavior from 25 to 1000 °C. Acta Mater. 2010;58(16):5326.

[4] Li JL, Cai GY, Zhong HS, Wang YX, Chen JM. Tribological properties in seawater for Ti/TiCN coatings on Ti6Al4V alloy by arc ion plating with different carbon contents. Rare Met. 2017;36(11):1.

[5] Shi ZT, Zhao HB, Chen XQ, Wu GM, Wei F. Chemical vapor deposition growth and transport properties of MoS$_2$–2H thin layers using molybdenum and sulfur as precursors. Rare Met. 2015. https://doi.org/10.1007/s12598-015-0599-x.

[6] Qu WT, Sun XG, Yuan BF. Tribological behaviour of biomedical Ti–Zr-based shape memory alloys. Rare Met. 2017;36(6):478.

[7] Muratore C, Voevodin AA. Molybdenum disulfide as a lubricant and catalyst in adaptive nanocomposite coatings. Surf Coat Technol. 2006;201(7):4125–30.

[8] Karthikeyan S, Jeeva PA, Arivazhagan N, Umasankar V, Srinivasan KN, Paramasivam M. Wear, hardness and corrosion resistance characteristics of tungsten sulfide incorporated electroless Ni–P coatings. Proced Eng. 2013;64(4):720.

[9] Redlich M, Gorodnev A, Feldman Y, Kaplanashiri I, Tenne R, Fleischer N, Genut M, Feuerstein N. Friction reduction and wear resistance of electro-co-deposited inorganic fullerene-like WS$_2$ coating for improved stainless steel orthodontic wires. J Mater Res. 2008;23(11):2909.

[10] Komarneni MR, Yu ZQ, Burghaus U, Tsverin Y, Zak A, Feldman Y, Tenne R. Characterization of Ni-coated WS$_2$ nanotubes for hydrodesulfurization catalysis. Isr J Chem. 2012;52(11–12):1053.

[11] Zhang WB, Liu XZ, Chen ZH, Chen D, Peng C. Latest development of WC-Co cemented carbide. Chin J Rare Met. 2015;39(2):178.

[12] Sivandipoor I, Ashrafizadeh F. Synthesis and tribological behaviour of electroless Ni–P–WS$_2$ composite coatings. Appl Surf Sci. 2012;263(48):314.

[13] Sangeetha S, Kalaignann PG. Tribological and electrochemical corrosion behavior of Ni–W/BN (hexagonal) nano-composite-coatings. Ceram Int. 2015;41(9):10415.

[14] Huang YS, Zeng XT, Hu XF, Liu FM. Corrosion resistance properties of electroless nickel composite coatings. Electrochim Acta. 2004;49(25):4313.

[15] Sun J, Li CS, Ji L, Tang H, Zhang Y, Li XC. Growth and mechanical properties of MoS$_2$/WS$_2$ composite films by magnetron sputtering. Chin J Vac Sci Technol. 2009;4(29):398.

[16] Zhou L, Yin GL, Wang YD, Yu Z, He DN. Tribological and wear properties of reaction-sputtered WS$_2$/MoS$_2$/C composite films. Chin J Nonferrous Met. 2010;3(20):483.

[17] Tsuru Y, Nomura M, Foulkes FR. Effects of boric acid on hydrogen evolution and internal stress in films deposited from a nickel sulfamate bath. J Appl Electrochem. 2002;32(6):629.

[18] Timoshkov I, Kurmashev V, Timoshkov V. Electroplated nanocomposites of high wear resistance for advanced systems application. In: Hashim A, editor. Advances in Nanocomposite Technology. Rijeka: InTech; 2011. 81.

[19] Kuo SL. The influence of process parameters on the MoS$_2$ content of Ni-MoS$_2$ composite coating by the robust design method. J Chin Inst Eng. 2004;27(2):243.

[20] Shrestha NK, Sakurada K, Masuko M, Saji T. Composite coatings of nickel and ceramic particles prepared in two steps. Surf Coat. 2001;140(2):175.

[21] EBRU Saraloğlu GÜLER. Electro co-deposition of molybdenum disulfide particles in nickel matrix. Ankara: Middle East Technical University; 2013. 22.

[22] Hui J, Zhu YW, Zhu CH, Liu YF. Dispersion characteristics of micro diamond particle in aqueous system. Diam Abras Eng. 2011;31(3):15.

[23] Tan CY. Fabrication of nickel, copper matrix composite coatings and their electrochemical behaviors. Changsha: Central South University; 2008. 4.

[24] Hou SX, Gao H, Jia XM. Research on friction property of WS$_2$ matrix solid lubricating coatings. Lubr Eng. 2013;4(38):82.

[25] Ma WL, Lu JJ. Effect of sliding speed on surface modification and tribological behavior of copper-graphite composite. Tribol Lett. 2011;41(2):363.

[26] Chen BM, Bi QL, Yang J, Xia Y, Hao J. Tribological properties of solid lubricants (graphite, h-BN) for Cu-based P/M friction composites. Tribol Int. 2008;41(12):1145.

[27] Kováčik J, Emmer Š, Bielek J, Keleši L. Effect of composition on friction coefficient of Cu-graphite composites. Wear. 2008; 265(3–4):417.

[28] Zhao YC, Xing HJ, Zhang ZW. The influence of lubricating phase MoS$_2$ on Ni60A composite coatings frictional characteristics. China Ceram. 2008;44(12):29.

[29] Wang XP, Xiao JK, Zhang L, Zhou KC. Effect of silver alloy particle size on friction and wear properties of Ag–MoS$_2$ composites. Chin J Nonferrous Met. 2012;22(10):2811.

[30] Lai DM, Tu JP, Zhang SC, Wang Q, Peng SM, He DN. Friction and wear properties of sputtered WS$_2$/Ag nanocomposite films in different environments. Tribology. 2006;6(26):515.

[31] Zheng C, Liu XB, Yang MS, Wang MD, Shi SH, Fu GY, Qi LH. High temperature self-lubricating wear-resistant NiCr–Cr$_3$C$_2$/30% WS$_2$ (Ni–P) composite coating fabricated by laser cladding. Trans Mater Heat Treat. 2013;34(6):136.